J Neurophysiol 120: 2011–2019, 2018.
First published August 22, 2018; doi:10.1152/jn.00488.2018.

RESEARCH ARTICLE | *Control of Movement*

Corticospinal correlates of fast and slow adaptive processes in motor learning

Adjmal M. E. Sarwary, Miles Wischnewski, Dennis J. L. G. Schutter, Luc P. J. Selen, and W. Pieter Medendorp

Radboud University, Donders Institute for Brain, Cognition and Behaviour, Nijmegen, The Netherlands

Submitted 18 July 2018; accepted in final form 20 July 2018

Sarwary AM, Wischnewski M, Schutter DJ, Selen LP, Medendorp WP. Corticospinal correlates of fast and slow adaptive processes in motor learning. *J Neurophysiol* 120: 2011–2019, 2018. First published August 22, 2018; doi:10.1152/jn.00488.2018.—Recent computational theories and behavioral observations suggest that motor learning is supported by multiple adaptation processes, operating on different timescales, but direct neural evidence is lacking. We tested this hypothesis by applying transcranial magnetic stimulation over motor cortex in 16 human subjects during a validated reach adaptation task. Motor-evoked potentials (MEPs) and cortical silent periods (CSPs) were recorded from the biceps brachii to assess modulations of corticospinal excitability as indices for corticospinal plasticity. Guided by a two-state adaptation model, we show that the MEP reflects an adaptive process that learns quickly but has poor retention, while the CSP correlates with a process that responds more slowly but retains information well. These results provide a physiological link between models of motor learning and distinct changes in corticospinal excitability. Our findings support the relationship between corticospinal gain modulations and the adaptive processes in motor learning.

NEW & NOTEWORTHY Computational theories and behavioral observations suggest that motor learning is supported by multiple adaptation processes, but direct neural evidence is lacking. We tested this hypothesis by applying transcranial magnetic stimulation over human motor cortex during a reach adaptation task. Guided by a two-state adaptation model, we show that the motor-evoked potential reflects a process that adapts and decays quickly, whereas the cortical silent period reflects slow adaptation and decay.

adaptation; CSP; force field; MEP; state-space model

INTRODUCTION

The behavioral mechanisms of motor learning have been studied extensively in the context of reach adaptation tasks in which individuals must learn to compensate for a systematic, visual, or mechanical perturbation (Krakauer et al. 2000; Shadmehr and Mussa-Ivaldi 1994). Traditionally, this adaptation is assumed to be driven by a single process (Scheidt et al. 2001; Thoroughman and Shadmehr 2000), but recent modeling and behavioral observations suggest that motor learning is governed by multiple interactive processes, operating on different timescales (Lee and Schweighofer 2009; Smith et al. 2006; Trewartha et al. 2014). Evidence is based on a paradigm that evokes spontaneous recovery—the reexpression of the initial adapted state, after it was followed by reverse-adaptation. This observation can be explained by a two-state adaptation model (Smith et al. 2006), suggesting that there are two adaptive processes in motor learning: a fast and a slow learning process. This two-state model of motor adaptation is not only able to explain spontaneous recovery but also the dynamics of learning (Anguera et al. 2009; Donchin et al. 2003), consolidation (Criscimagna-Hemminger and Shadmehr 2008), and interference (Sing and Smith 2010), even in particular patient groups (de Werd et al. 2013).

While various brain regions have been implicated in motor learning, including the cerebellum, posterior parietal cortex, premotor cortex, and primary motor cortex (M1), the physiological correlate of a two-state model remains inconclusive. In monkey M1, Mandelblat-Cerf et al. (2011) reported different dynamics of neural changes during adaptation to force-field perturbations. While this can be taken as evidence that M1 can accommodate slow and fast learning processes, the authors observed these different neuronal dynamics during different learning schedules, not during a single schedule. In humans, Kim et al. (2015) performed a functional MRI experiment in which subjects adapted to two opposing visuomotor rotations. Using a model-based analysis approach, they demonstrated the existence of separate neural circuits with different timescales for adaptation, but they could not directly probe the interacting neural processes during the course of motor adaptation.

The search for direct cortical evidence of the two-state learning model is challenging. Learning mechanisms depend on synaptic plasticity and efficacy, modulated by excitatory and inhibitory neuronal circuits (Terao and Ugawa 2002) that drive long-term potentiation and long-term depression (Dayan and Cohen 2011; Fusi et al. 2007; Rioult-Pedotti et al. 2000). With regard to the M1, its excitability can be measured using electromyographic recordings of the motor-evoked potential (MEP) in response to single-pulse transcranial magnetic stimulation (TMS) (Bestmann and Krakauer 2015; Ziemann 2004). The MEP represents the weighted sum of excitatory and inhibitory postsynaptic potentials and is a noninvasive measure of corticospinal excitability (Bachtiar and Stagg 2014; Bestmann and Krakauer 2015; Di Lazzaro and Ziemann 2013). It also known that, during voluntary muscle contractions, there is a period of electromyographic suppression following the MEP (Garvey et al. 2001), known as the cortical silent period (CSP). In addition to spinal contributions, the CSP is assumed to index intracortical $GABA_B$-mediated inhibitory mechanisms (Terao and Ugawa 2002; van den Wildenberg et al. 2010).

Address for reprint requests and other correspondence: W. P. Medendorp, Radboud Univ., Donders Institute for Brain, Cognition and Behaviour, Nijmegen, 6525 HR, The Netherlands (e-mail: p.medendorp@donders.ru.nl).

Various studies have shown that the MEP follows the motor output during early learning but readily returns to baseline while the output can be maintained (Bagce et al. 2013; McDonnell and Ridding 2006). The latter is proposed to reflect a GABA-ergic mediated inhibitory mechanism that may occur during later learning phases linked to retaining the motor memory trace (Spampinato and Celnik 2017). With these notions in mind, it can be hypothesized that the modulations of MEP and CSP during learning are indices of corticospinal excitability with fast and slow dynamics, respectively. Therefore, using a model-guided analysis, we investigated in this study whether the human motor cortex contains signatures of the two-state adaptation model, and, hence, reflects its neural basis.

MATERIALS AND METHODS

Participants

Twenty-four healthy right-handed volunteers participated in the study, which was performed in accordance with the standards set by the Declaration of Helsinki, and the protocol was approved by the Committee on Research Arnhem-Nijmegen, The Netherlands. Inclusion criteria for participants were that they must be right-handed (mean Oldfield score ± SE, 82.94 ± 5.48) and have normal or corrected-to-normal vision. Exclusion criteria were disorders of the visual and motor system, metal in cranium, use of medication (i.e., antiepileptics, antidepressants, neuroleptics, or benzodiazepines), first-degree epilepsy or family history of epilepsy, history of closed-head injury, history of head surgery, history of neurological or psychiatric disorders, medication pump, brain infarction, heart disease, cardiac pacemaker, pregnancy, and electronic hearing devices. Written informed consent was obtained, and they received payment for participation. Eight subjects were excluded because their resting motor threshold was too high (see *Procedure*), such that 16 participants (28 ± 1.3 yr; 10 men and 6 women) performed the actual experiment.

Apparatus and Setup

Robotic manipulandum. Subjects were seated on a height-adjustable chair in front of a robotic rig (Fig. 1*A*). Their right arm rested on an air sled floating on a glass top table. Reaches were performed in the horizontal plane while holding the handle of a planar robotic manipulandum (Howard et al. 2009). Handle position and forces at the handle were measured and controlled at 1,000 Hz. Stimuli were presented within the plane of movement via a semi-silvered mirror, which also allowed visual feedback of hand position to be overlaid into the plane of the movement. Subjects were prevented from viewing their arm directly.

Electromyographic recordings. Surface electromyographic (EMG) activity was recorded from the biceps brachii (BB), using wireless active sensors, which include a reference and ground (Delsys Trigno). Signals were sampled at 1,111 Hz, hardware band-pass filtered over a bandwidth of 20–450 Hz.

Transcranial magnetic stimulation. Biphasic single-pulse TMS was applied with a Magpro-X-100 magnetic stimulator and a MC-B65 figure-of-eight coil (outer diameter: 75 mm) (MagVenture, Hückelhoven, Germany). The stimulation coil was placed tangentially on the scalp with its handle pointing in a posterior direction and laterally at an angle of ~45° away from midline (Werhahn et al. 1994). The surface hotspot for the biceps brachii was tracked using the Localite neuronavigation system (Localite, Sankt Augustin, Germany). During the experiment, coil location was continuously monitored and kept constant within a range of <2 mm displacement and <2° rotation).

Procedure

Each experiment consisted of an intake session (35 min) and an experimental session (75 min). During the intake session, safety issues and experimental procedures were explained. Individuals were screened (~10 min) for contraindications to TMS (Keel et al. 2001), and right-handedness was assessed (Oldfield 1971). Before the experiment, participants received the instructions to refrain from taking psychotropic substances. After informed consent was obtained, EMG electrodes and neuro-navigation sensors were attached (~10 min), and the participant was seated in front of the manipulandum resting the right arm on an air sled. Next, resting motor threshold (rMT) of the right biceps brachii was obtained for establishing a subject-specific

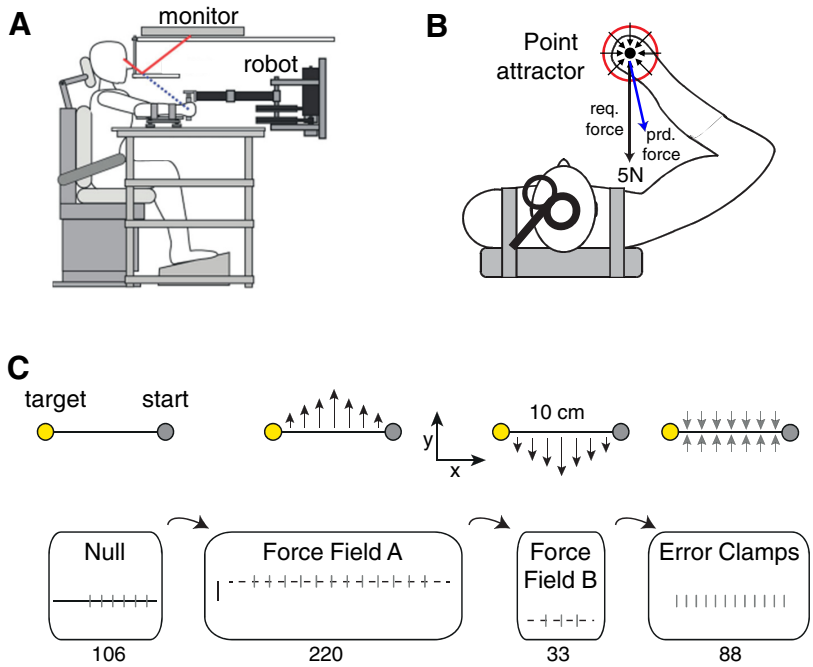

Fig. 1. Experimental paradigm. *A*: robotic manipulandum with the arm supported by an airsled. *B*: configuration for eliciting motor-evoked potentials (MEPs), which were measured interspersed with the reach trials. *C*: trial sequence of the paradigm and reach direction. Every vertical bar denotes an error-clamp trial. The start position (gray circles, 1.5-cm radius) and target position (yellow circles, 1.5-cm radius) were simultaneously displayed. A red cursor (0.5 cm radius) indicated the hand position.

stimulation intensity (~15 min). rMT was defined as the minimum intensity to elicit a motor-evoked potential (MEP) amplitude of >0.05 mV in at least 5 out of 10 trials and was determined to the nearest percentage of maximum stimulator output (Rossini et al. 2015).

Eight subjects were excluded from the study because the resting motor threshold of the biceps brachii was too high, exceeding the maximum stimulator output at 120% rMT in the experimental session. For the remaining subjects, after the rMT for the biceps brachii was obtained, the stimulation location was marked in the neuro-navigation system. These subjects had a mean rMT of 64.7 ± 3.1 (SE) and performed the actual experiment in ~75 min, following the protocol below.

Reach Task

Subjects had to perform 10-cm reaching movements in the frontal plane, from right to left (Fig. 1*C*), to use the biceps brachii as target muscle from which the electromyographic recordings were measured. The start position (in gray, 1.5-cm radius) and target position (in yellow, 1.5-cm radius) were simultaneously displayed. A red cursor (0.5 cm radius) indicated the hand position. Before the start of the trial, the subject had to place the hand cursor within the start position and stay still (cursor speed <5 cm/s for 100 ms). Then, a tone instructed the subject to start the reach. If the reach was initiated before the tone or started >1 s after the tone, subjects received an error message, and the trial was repeated. The end point of the movement was defined as the first point where the speed <5 cm/s. If this end point was anywhere within the target area, the target turned from yellow to green. If the end point was not within the target region or the reach lasted longer than 500 ms, a feedback message was given. These feedback messages were used to make the reaches more consistent but did not lead to rejection of the trial.

During the reach, the robot motors could be off (null), produce a curl force field [clockwise (CW) or counterclockwise], or produce an error-clamp (Scheidt et al. 2000; Smith et al. 2006). In a curl force field, forces are produced that are perpendicular to movement direction and proportional to the reach velocity: $F_x = -b \cdot v_y$ and $F_y = b \cdot v_x$, with the damping constant b set to ± 13·N·s/m. The sign of b determined the direction of the force field, with a negative damping constant associated with a CW field. Error-clamp trials constrained the movement onto a straight line from the start to the target position, using a spring constant of 6,000 N·m and a damping constant of 7.5 N·s/m. Error-clamps served to measure the adaptation index (AI). Both the curl force fields and error-clamps were initiated at the onset of the tone that signaled the start of the reach.

At the end of the reach, subjects were instructed to relax their arm, while the robot returned the hand to the start position. This passive return movement followed a minimum jerk profile with a duration of 700 ms. The hand was pulled onto this trajectory by a PD controller with a spring constant of 3,000 N·m and a damping constant of 2.5 N·s/m.

Protocol

Subjects performed reaches following a protocol that consisted of four blocks (Fig. 1*C*): a baseline phase (106 null trials), long adaptation phase (220 trials, clockwise force field), short adaptation phase (33 trials, counterclockwise force field), and an error-clamp block (88 trials). The amount of learning during the first three blocks was quantified by interspersing an error-clamp trial within every five reach trials. The fourth block only contained error-clamp trials (Scheidt et al. 2000).

Throughout the last three blocks, a brief TMS session was performed after every 10 reach trials, during which the hand was kept still. In the baseline phase, allowing for a long familiarization phase to the robot, the TMS session followed after every 20 reaches to perform no more TMS sessions than needed. In total, there were 37 TMS sessions across the four blocks. In the TMS session, the subject produced a constant isometric force of 5 N in the midsagittal plane (i.e., <5% maximal voluntary contraction) toward their body, while the robot clamped the hand into a predefined position (stiffness constant: 9,000 N·m). Thus, the biomechanical state (kinematics and force) was the same in all TMS trials, and the changes in MEP and CSP were measured under a fixed load of the muscle. Subjects received visual feedback about the required (black) and actual (blue) force direction and magnitude by displaying force vectors on screen (see Fig. 1*B*). If the force vectors matched within the tolerances (±0.5 N and ±15°), the screen turned green, otherwise it stayed red (see Fig. 1*B*).

TMS pulses were initiated by software controlling the experiment and were only delivered if the required and produced force were within the tolerances. Each TMS session contained 10 single TMS pulses over left M1, separated by 5,000–7,000-ms intervals, to evaluate the time course of the MEP and CSP of the right biceps brachii. Stimulation intensity was 120% of the individual's rMT (Schutter and van Honk 2006).

Data Analysis

All data were stored for offline analysis in MATLAB (The MathWorks). From the error-clamp trials, we computed an AI representing the fraction of ideal force compensation. To this end, on the basis of the velocity of the handle along the channel, we calculated the theoretical time-varying force generated by the curl field. This theoretical force was regressed against the force measured in the error-clamp, providing a regression coefficient (AI) in the range of −1 to 1 (see Joiner and Smith, 2008 for a detailed illustration). For the adaptation blocks, the AIs were signed on the basis of the force field direction to separate the compensatory forces for the CW and CCW curl fields. We fitted a two-state adaptation model (Smith et al. 2006) to capture the time course of the AI. This model specifies a fast and slow parallel learning process, each of which depends on the learning at the previous trial (k) multiplied by a retention factor (R) and the error (e) during that trial multiplied by the learning rate (L), following:

$$e(k) = f(k) - x_{\text{net}}(k)$$
$$ex_{\text{fast}}(k+1) = R_{\text{fast}} \cdot x_{\text{fast}}(k) - L_{\text{fast}} \cdot e(k)$$
$$x_{\text{slow}}(k+1) = R_{\text{slow}} \cdot x_{\text{slow}}(k) - L_{\text{slow}} \cdot e(k)$$
$$x_{\text{net}}(k+1) = x_{\text{fast}}(k+1) + x_{\text{slow}}(k+1)$$

where x_{fast} and x_{slow} represent the outputs of the fast and slow learning processes, respectively. The error e is calculated on the basis of the applied perturbation force (f) and the motor output (x_{net}). The initial value of x_{net} was set to zero; parameters were constrained following $R_{\text{fast}} < R_{\text{slow}} < 1$ and $L_{\text{fast}} > L_{\text{slow}} > 0$. This model was fit on an individual subject basis, providing four fit parameters per subject. Fitting was performed using MATLAB function "fmincon".

A single TMS session consisted of 10 pulses. The evoked EMG traces of these pulses were averaged, aligned to pulse onset, and subsequently analyzed for MEP amplitude and CSP duration (see Fig. 2*A*). The peak-to-peak amplitude of the MEP was defined on the basis of the peak and trough of the waveform. Using a custom-written MATLAB program (cf. Garvey et al. 2001; Rábago et al. 2009), CSP duration was determined as the time from TMS onset to the time of reappearance of the EMG signal, determined as an average across the 10 trials of the session, which was more than twofold the SD of the background EMG noise at rest (see Kojima et al. 2013 for a similar approach). Results were visually inspected by two experimenters and corrected as needed.

The individually fitted model provides a time course for the AI accounted for by the fast and slow state, so also at the time of the TMS trial. The fast and slow process states were correlated to the MEP amplitude and CSP duration of the individual subjects. We also fitted

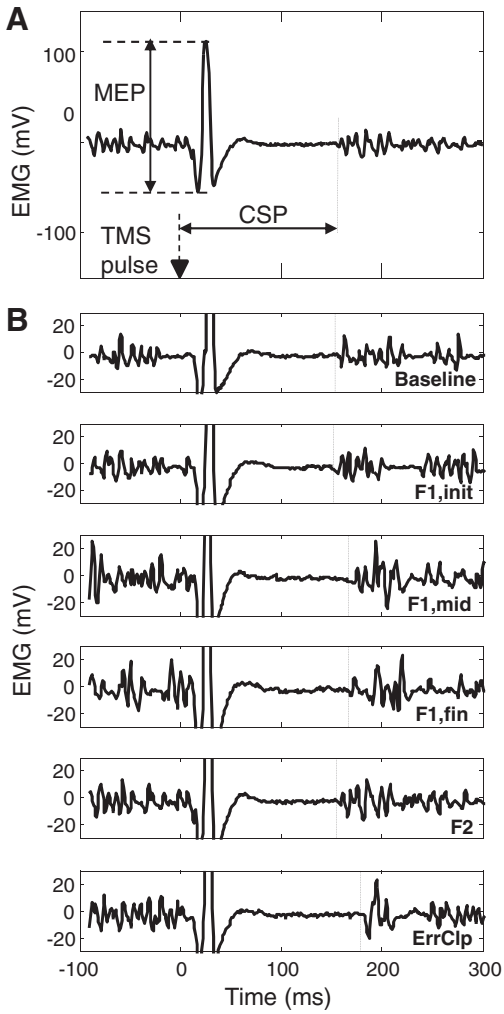

Fig. 2. *A*: example EMG trace of biceps brachii around the TMS pulse application ($t = 0$). MEP magnitude and CSP duration are indicated. *B*: cortical silent period (CSP) duration of a single subject for different trials of the paradigm (baseline, *field 1*, initial trial, middle trial, and final trial, *field 2*, and an error clamp trial) in a single subject.

one-state, single-rate models to the MEP and CSP, respectively, to check whether these dynamics correspond to the putative dynamics, as suggested by the two-state model of AI. To assess significance levels, we used within-subject ANOVAs, and individual correlation coefficients were tested against zero using one-sample *t*-tests.

RESULTS

Reaches were made from right to left in the frontal plane, using a protocol consisting of four blocks (Fig. 1*C*). A baseline phase was followed by a long adaptation phase in CW force field (CW field). This was followed by a short adaptation phase to a counterclockwise (CCW) force field before the final error-clamp block began.

Force Field Learning and Spontaneous Recovery

To quantify learning, within the first three blocks, every fifth trial was an error-clamp trial, in which the robot clamped the reach to a straight line, while the compensatory force was measured (Scheidt et al. 2000). All trials in the fourth-block were error-clamps. We computed an AI representing the fraction of ideal force compensation (Joiner and Smith 2008). Figure 3*A*, *top*, shows the adaptation index (black circles) over the course of the experiment in a typical subject; Fig. 3*B*, *top*, shows the mean behavioral adaptation across subjects. For the latter, a within-subject ANOVA revealed a significant effect of trial number [$F(384,2656) = 14.1$, $P < 0.0001$].

As shown, force expression is small and unsystematic during the baseline phase, as expected since the robot did not perturb the reaches in this block. However, during the CW learning block, the AI gradually increases as subjects learn to compensate for the forces applied by the robot, approaching perfect compensation at the asymptotic level. This means that at the end of the CW learning block, the force employed by the reach cancels the forces applied by the robot. During the subsequent CCW block, when the force field has switched to the opposite direction, the AI quickly returns to baseline levels and switches sign while starting to compensate for the CCW force field. Next, during the final error-clamp block, the AI rapidly rebounds, as shown in both the single subject and the average across subjects, expressing, at least in part, the compensatory strategy for the initial, CW force field. This rebound is known as spontaneous recovery (Kojima et al. 2004; Smith et al. 2006), which slowly declines to baseline performance.

Inferring Adaptive States

We fitted a two-state adaptation model (Smith et al. 2006) to capture the time course of the AI (see MATERIALS AND METHODS). Fig. 3, *A* and *B*, *top*, depict the two components of the model, showing the state of the fast process (in red), which learns and decays quickly, and the slow process (in blue), which learns and decays slowly. The model's estimate of the external forces is governed by the summed states of these processes, $x_{fast} + x_{slow}$ (black line) and provides a strong correspondence with the behaviorally observed force expression ($r = 0.92$, $P < <0.001$ across subjects; see Fig. 3*B*). Upon closer inspection, the model slightly underestimates the amplitude of the rebound and does not fully capture the slight decay during the spontaneous recovery. Yet, for the single subject shown, and the other individual subjects, the model generally provided a very good fit (with $0.84 < r < 0.98$ for individual subjects, $t(445) > 32.0$, all $P < 0.001$).

The best-fit model parameters were consistent across subjects, with $R_{fast} = 0.77$ (0.12 SD), $L_{fast} = 0.16$ (0.10 SD), $R_{slow} = 0.99$ (<0.001 SD), and $L_{slow} = 0.02$ (0.01 SD). These values were in the same range as reported by previous studies (Smith et al. 2006; Trewartha et al. 2014). Importantly, according to the two-state model, the quick learning of the CCW field is driven by the fast process, whereas the reexpression of the compensatory strategy of CW field in the error-clamp block is caused by the slow process that has not yet transitioned to compensate for the CCW field.

Corticospinal Correlates of Adaptive States

We assessed changes in cortical plasticity with brief TMS sessions interspersed throughout the paradigm, during which the hand did not move. After every 10 reach trials (every 20 ms in the baseline phase), a short series of 10 single TMS pulses (interpulse interval 5,000–7,000 ms) was applied to the left motor cortex, to evaluate corticospinal excitability levels (Fig. 2*A*).

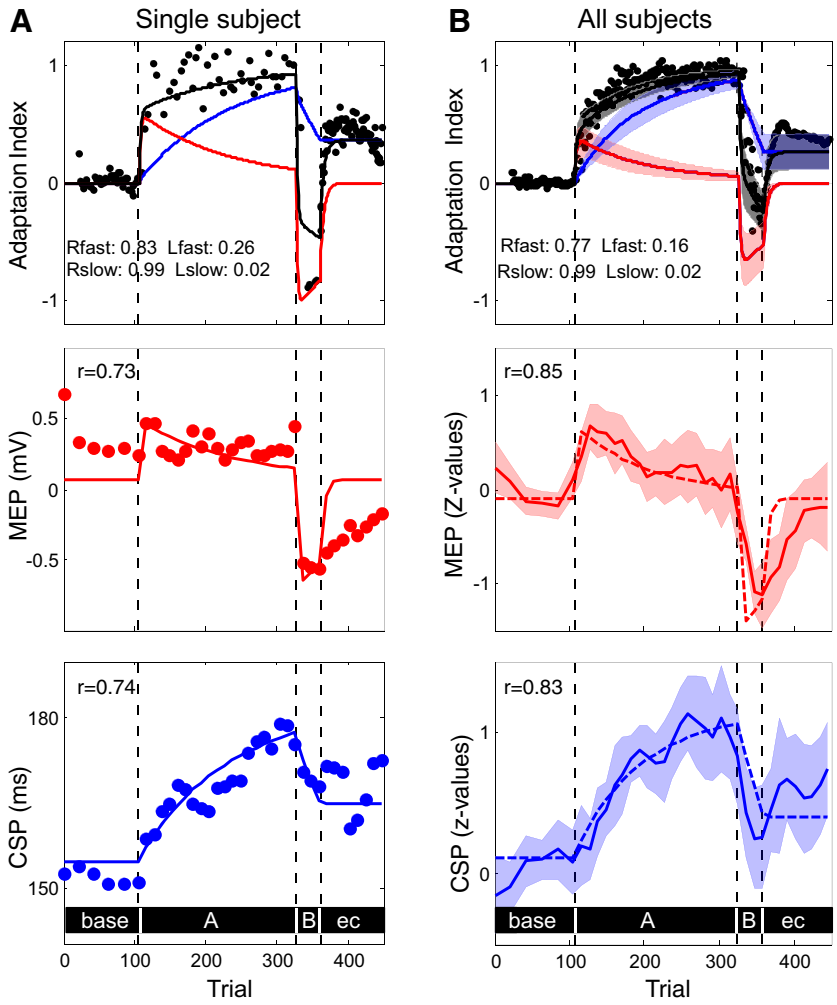

Fig. 3. Adaptation index, fast and slow process contributions, and physiological proxies [motor-evoked potential (MEP) amplitude, and cortical silent period (CSP) duration] across trials, in a single subject (*A*) and as an average ± SE across subjects (*B*). *Top*: evolution of adaptation index (AI; black dots). A two-state adaptation model was fitted to the behavioral data (black line), with a fast (red line) and slow (blue line) component. Fit parameters are indicated. *Middle*: sign-normalized MEP of the individual transcranial magnetic stimulation (TMS) sessions together with a scaled version of the average fast process. Correlation coefficients are indicated. MEPs are shown as *z*-scores in the calculation of the average across subjects. *Bottom*: CSP duration of the individual TMS sessions together with a scaled version of the average slow process. Correlation coefficients are indicated. CSP expressed as *z*-scores for the average.

Peak-to-peak amplitude of the MEP (see Fig. 2*A*) is a measure of corticospinal excitability. Figure 3*A*, *middle*, shows the MEP amplitude as a function of trial number in the typical subject; Fig. 3*B*, *middle*, demonstrates the mean MEP amplitude across subjects, expressed in *z*-score values (± SE). Note that, because the MEP is only sensitive to learning-related changes, its size cannot become negative if the force field changes direction. Therefore, we signed the normalized MEP values based on the sign of the individual subject's fitted fast process, resulting in the sign-normalized MEP. A within-subject ANOVA revealed a significant effect of trial number [$F(36,555) = 2.8$, $P < 0.001$].

Fig. 3, *middle*, shows that during the first baseline block, the amplitude of the MEP is relatively stable. Across subjects, across the six MEP measurements that were taken during this block, the MEP amplitude did not change significantly [ANOVA, $F(5,90) = 2.0$, $P = 0.08$], suggesting that the MEP amplitude changes are not related to task performance per se, but to learning as the subsequent trials show. During the block with CW learning trials, the MEP amplitude first increases, but then gradually declines when the learning block proceeds. During the subsequent CCW block, MEP amplitude (now signed negatively following the sign of fitted fast process) quickly increases again, and during the error-clamp block, MEP amplitude returns rapidly to baseline levels. This MEP amplitude pattern is remarkably similar to the time course of the fast process, which is overlaid, and independently inferred from the behavioral data based on the model fit. Any difference with its predicted time course seems to occur during the spontaneous recovery period, when the MEP decays slightly slower than predicted. The correlation coefficient between MEP pattern and the model's fast process components was 0.73 [*t*-test, $t(35) = 6.3$, $P < 0.001$] for the single subject shown. The correlation coefficients varied between 0.51 and 0.76 across subjects ($P < 0.05$ in 16 of 16 subjects) and was 0.85 ($P < 0.001$) when data were averaged across subjects, suggesting that MEP amplitude can be taken as a proxy of the fast adaptation process in motor learning. Of note, we also tested the correlation between the unsigned MEP and the unsigned time course of the fast process, which still revealed a highly significant correlation across subjects ($r = 0.7$, $P < 0.001$).

As depicted in Fig. 2*A*, the MEP is followed by the CSP, due to a transient $GABA_B$-mediated suppression of EMG activity (Di Lazzaro and Ziemann 2013; Ziemann et al. 2008). Figure 2*B* shows the duration of the CSP (in the order of 150–180 ms) during the different phases of the paradigm for a typical subject. Detailed observations reveal small changes in the duration of the CSP over the course of the experiment. Compared with baseline, the duration of the CSP appears to increase slightly during the first, longer-lasting force field, and

then decreases during the shorter period of the second force field, after which it increases again.

These results are summarized in Fig. 3*A*, *bottom*, for a single subject (blue circles), and in Fig. 3*B*, *bottom*, as a *z*-score-based average across subjects (means ± SE). A within-subjects ANOVA revealed a significant effect of trial number [$F(36,555) = 1.8$, $P = 0.004$]. As shown, during the CW learning block, duration of the CSP gradually becomes longer, reaching almost a plateau at the end. When the force field switches, the CSP duration declines slightly (but does not completely drop back to baseline) and remains relatively constant during the error-clamp block. This CSP pattern significantly correlates with the slow-phase component, as inferred from the model fit to the behavioral data in the single subject [$r = 0.74$, $t(35) = 6.5$, $P < 0.001$], and was $r = 0.83$ ($P < <0.001$), when data were averaged across subjects. The correlation coefficient varies between 0.06 and 0.76 for an individual subject ($P < 0.05$ in 12 of 16 subjects). This suggests that the CSP is a proxy of the slow adaptation process in motor learning.

Although MEP amplitude, CSP duration, and AI have different units of measurement, we tested whether a linear combination of the first two signals, normalized based on their peak, can explain the changes of the AI during the course of the experiment. Figure 4*A* shows that the aggregated time course, superimposed on the mean data across subjects, captures the dynamic changes of the AI very well. Figure 4*B* shows that the aggregate time course has a significant correlation with the time course of the AI [$r = 0.84$, $t(35) = 9.2$, $P < 0.001$]. This suggests that the MEP and CSP are markers that reflect the internal states of two adaptive processes, which only in combination explain the behavioral output of the system.

To further characterize the dynamics of the MEP and CSP, we fitted explicit one-state models to their time course, and compared their fit parameters to the independently obtained parameters of the two-state model fit to the behaviorally obtained AI. Note that, compared with fits to AI, the one-state fits are based on limited data points (37 MEP/CSP values per subject). Because this could explain some outliers in the best-fit parameters (three subjects settled the retention rate on the lower bound of zero), we took the median (±IQR) to characterize the subject group. Table 1 shows the result, indicating that one-state models of the MEP and CSP nicely correspond to the fast and slow processes of the two-state model of AI.

Inspired by the two-state learning theory, we also tested two further predictions. Given that the slow process is primarily responsible for the spontaneous recovery, the CSP at the end the first force field should correlate with the amount of spontaneous recovery observed behaviorally (AI) and with the CSP during that period (thus, the AI and CSP at the end of the error clamp period, respectively). Although the first correlation was not significant ($r = 0.43$, $P = 0.09$), the second correlation was significant ($r = 0.63$, $P = 0.004$), which does not allow a straightforward interpretation, perhaps because the analyses are based on a limited number of subjects.

Finally, we performed several control analyses. First, we checked for fatigue effects by examining whether the baseline EMG level before the TMS pulse changes over the course of the experiment. Across subjects, we did not find a significant relationship [slope = 0.01 ± 0.04 μV/trial (mean ± SD), *t*-test, $t(15) = 1.5$, $P = 0.17$, 95% CI [−0.01, 0.03] μV/trial]. We also found no significant relationship between the level of EMG activity before the TMS pulse and the subsequent MEP size [slope = $-4{\cdot}10^{-11} \pm 5{\cdot}10^{-10}$, *t*-test, $t(15) = 0.3$, $P = 0.76$, 95% CI [$-2.9{\cdot}10^{-11}$, $2.1{\cdot}10^{-11}$]] or CSP duration [slope = 0.3 ± 1.0 μV/s, *t*-test, $t(15) = 1.2$, $P = 0.24$, 95% CI [−0.2, 0.8] μV/s]. In all cases, the small confidence intervals, including zero, show that these null results exclude effects of any real interest and suggests that the MEP or CSP modulations cannot be explained by fatigue-related or other nonspecific changes in tonic EMG activity, before the TMS pulse (Rodi and Springer 2011).

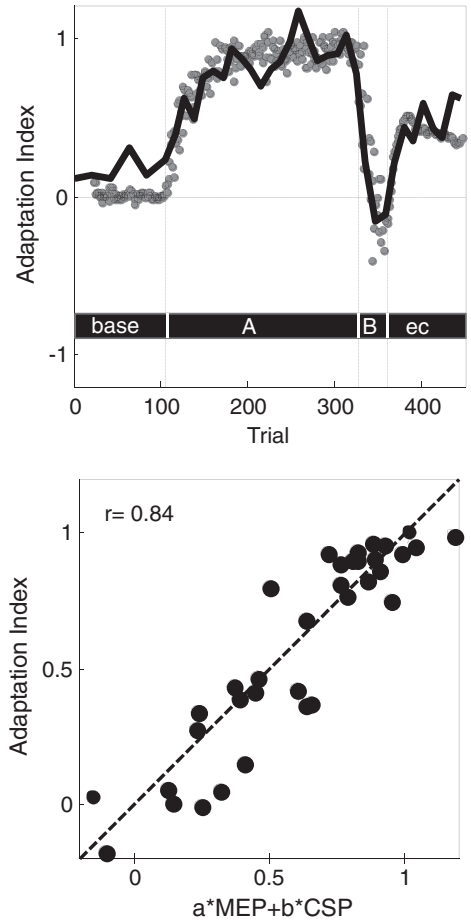

Fig. 4. *A*: aggregated time course (black line), based on a linear combination of the motor-evoked potential (MEP) and cortical silent period (CSP), superimposed on the mean data (gray circles) across subjects. *B*: correlation between the dynamic changes of the adaptation index (AI) and the predicted change based on the aggregated time course.

DISCUSSION

Using TMS in combination with EMG, we measured the MEP and the CSP in the biceps muscle during sessions of isometric contractions, which intervene in an established motor learning protocol that evokes spontaneous recovery. Guided by a two-state adaptation model, we examined physiological evidence of the slow and fast learning processes in motor learning.

Our results show that MEP amplitude is not related to the motor output itself in a learning process (Bagce et al. 2013; McDonnell and Ridding 2006), but rather suggest that it

Table 1. *One and two-state model fits to AI, MEP, and CSP*

	Fast Process		Slow Process	
	R (means ± SD)	*L* (mean ± SD)	*R* (means ± SD)	*L* (means ± SD)
Two-State Model				
AI	0.77 (0.12)	0.16 (0.10)	0.99 (0.0002)	0.02 (0.01)
One-State Model				
	R (median ± IQR)		*L* (median + IQR)	
MEP	0.77 (0.34)		0.08 (0.05)	
CSP	0.96 (0.46)		0.03 (0.03)	

AI, adaptation index; CSP, cortical silent period; IQR, interquartile range; *L*, learning rate; MEP, motor-evoked potentials; *R*, retention factor. Parameters of one-state model fits are the median ± IQR, to deal with outlier values (see main text).

represents the internal state of a fast learning process and is only one part of the motor output. Similarly, CSP modulation is not correlated to the motor output, but it is related to the state of a slow learning process that forms the second part of the total motor output. Importantly, our results do not argue against the notion that even more interacting adaptive processes, with different timescales, underlie short-term motor learning (Kim et al. 2015; Lee and Schweighofer 2009). However, we can only speculate whether or not such additional adaptive processes explain the characteristics of the MEP and CPS that could not be accounted for by the two-state model.

It has been proposed that single-pulse TMS over the primary motor cortex produces direct activation of the excitatory glutamatergic pyramidal neurons in *layers 2* and 3, as well as the larger pyramidal tract neurons in output *layer 5*, and the inhibitory GABAergic interneurons that synapse on pyramidal neurons (Di Lazzaro and Ziemann 2013). During learning, we propose that this microcircuitry of the motor cortex reorganizes and synaptic efficacy changes, mediated by $GABA_B$ type receptors, supposedly operating via LTP/LTD-dependent synaptic strengthening of cortical horizontal connections (Hess and Donoghue 1994; Monfils et al. 2004). These processes are not likely to operate in isolation and can also be shaped by subcortical brain areas, like the cerebellum (Kishore et al. 2014) and cortico-cortical pathways (Bestmann et al. 2008; Hamada et al. 2014).

Changes in MEP amplitude may, thus, reflect a compound signal that is a read-out of the state of postsynaptic cortical excitability and presynaptic intracortical processes, possibly reflecting the fast learning process. In a follow-up of this work, one could use paired-pulse TMS to further disambiguate this signal (Hallett 2007). Recent reports have implicated strategic learning in the fast process of motor adaptation (Huberdeau et al. 2015; Taylor and Ivry 2014), perhaps through the involvement of the prefrontal cortex. Empirical data suggest that prefrontal activation mostly arises during the early stages of learning (Anguera et al. 2010; Seidler and Noll 2008). Although we did not provide explicit information about the perturbations to our subjects, it can be speculated that frontal-cortical loops govern the fast and cognitively mediated early response and that the observed MEP changes reflect in essence a read-out of these loops.

Cortical inhibition has been associated with the occlusion of synaptic plasticity (Ziemann and Siebner 2008), which is known to occur late during learning to retain the newly formed memory (Spampinato and Celnik 2017). Inhibitory cortical processes, as probed by the CSP, could modulate the MEP amplitude. Although we did not find a significant correlation between MEP amplitude and CSP duration ($r = -0.03$, $t(590) = -0.77$, $P = 0.44$), we do not suggest that MEP and CSP should merely be viewed as proxies for completely decoupled neural systems.

Although our data provide physiological evidence for the existence of the two learning processes, it is important to point out that they do not yet constitute causal proof. For example, one could suppose that the observed MEP and CSP manifest themselves through a nonlinear transformation of single-state dynamics, neglecting a hidden constraint. Also, although both signals are derived from stimulating the motor cortex, we cannot exclude that they reflect a downstream effect driven by a learning process that is, in fact, located more upstream in the sensorimotor system.

It is well established that the cerebellum is also involved in motor learning (Celnik 2015; Izawa et al. 2012; Taylor and Ivry 2014;). Patients with cerebellar damage show deficits in reach adaptation (Bhanpuri et al. 2014; Maschke et al. 2004). Some have suggested that the cerebellum is responsible for the actual learning, whereas M1 is responsible for consolidating what the cerebellum has learnt (Galea et al. 2011; Hadipour-Niktarash et al. 2007). One interpretation of this result might be that the cerebello-cortical loop supports the fast learning process, while the motor cortex is involved in the slow process. However, the parsimonious interpretation of our results is that both processes are located in the motor cortex. Whether some of the processes, in fact, reflect a corollary from processes that are actually implemented in the cerebellum or other structures requires further study.

Although it has been suggested that muscle fatigue affects corticospinal excitability during adaptation (Taylor et al. 1996), we do not think that this can explain our results. First, the sustained contractions of the muscle during the baseline were relatively minor, estimated to be <5% of the maximum voluntary contraction (MVC) for a duration of 1 min. Fatigue effects on the MEP are only reported at >30% MVC, typically showing an increase in size of the MEP, whereas we see a decrease during the learning in first force block. The CSP has been reported to increase in duration but only during sustained contraction of >30% MVC, which is far above our % MVC values (Taylor et al. 1996). Furthermore, we validated that the baseline EMG level before the TMS pulse did not change significantly over the course of the experiment, and we neither observed a significant correlation between the level of EMG activity before the TMS pulse and the subsequent MEP size or CSP duration. Finally, our findings cannot be explained by differences in TMS intensity and muscle contraction force, as they were kept constant throughout the experiment.

In conclusion, this study provides a neural correlate for a behaviorally derived two-state adaptation process. We found that the modulations of MEP amplitude and CSP duration are proxies of dedicated processes in the motor cortex and downstream regions that express different sensitivities to learning and retention, reflecting the fast and slow component of a two-state adaptation process. Our findings contribute to under-

standing the relations between corticospinal gain modulations and processes associated with coding memory states in motor learning.

GRANTS

This work was supported by an internal grant from the Donders Centre for Cognition and by grants from the European Research Council (EU-ERC-283567) and the Netherlands Organization for Scientific Research (NWO-VICI: 453–11–001) to W. P. Medendorp.

DISCLOSURES

No conflicts of interest, financial or otherwise, are declared by the authors.

AUTHOR CONTRIBUTIONS

A.M.S., D.J.S., L.P.S., and W.P.M. conceived and designed research; A.M.S. and M.W. performed experiments; A.M.S., L.P.S., and W.P.M. analyzed data; A.M.S., D.J.S., L.P.S., and W.P.M. interpreted results of experiments; A.M.S. and W.P.M. prepared figures; A.M.S. and W.P.M. drafted manuscript; A.M.S., M.W., D.J.S., L.P.S., and W.P.M. edited and revised manuscript; A.M.S., M.W., D.J.S., L.P.S., and W.P.M. approved final version of manuscript.

REFERENCES

Anguera JA, Reuter-Lorenz PA, Willingham DT, Seidler RD. Contributions of spatial working memory to visuomotor learning. *J Cogn Neurosci* 22: 1917–1930, 2010. doi:10.1162/jocn.2009.21351.

Anguera JA, Seidler RD, Gehring WJ. Changes in performance monitoring during sensorimotor adaptation. *J Neurophysiol* 102: 1868–1879, 2009. doi:10.1152/jn.00063.2009.

Bachtiar V, Stagg CJ. The role of inhibition in human motor cortical plasticity. *Neuroscience* 278: 93–104, 2014. doi:10.1016/j.neuroscience.2014.07.059.

Bagce HF, Saleh S, Adamovich SV, Krakauer JW, Tunik E. Corticospinal excitability is enhanced after visuomotor adaptation and depends on learning rather than performance or error. *J Neurophysiol* 109: 1097–1106, 2013. doi:10.1152/jn.00304.2012.

Bestmann S, Krakauer JW. The uses and interpretations of the motor-evoked potential for understanding behaviour. *Exp Brain Res* 233: 679–689, 2015. doi:10.1007/s00221-014-4183-7.

Bestmann S, Swayne O, Blankenburg F, Ruff CC, Haggard P, Weiskopf N, Josephs O, Driver J, Rothwell JC, Ward NS. Dorsal premotor cortex exerts state-dependent causal influences on activity in contralateral primary motor and dorsal premotor cortex. *Cereb Cortex* 18: 1281–1291, 2008. doi:10.1093/cercor/bhm159.

Bhanpuri NH, Okamura AM, Bastian AJ. Predicting and correcting ataxia using a model of cerebellar function. *Brain* 137: 1931–1944, 2014. doi:10.1093/brain/awu115.

Celnik P. Understanding and modulating motor learning with cerebellar stimulation. *Cerebellum* 14: 171–174, 2015. doi:10.1007/s12311-014-0607-y.

Criscimagna-Hemminger SE, Shadmehr R. Consolidation patterns of human motor memory. *J Neurosci* 28: 9610–9618, 2008. doi:10.1523/JNEUROSCI.3071-08.2008.

Dayan E, Cohen LG. Neuroplasticity subserving motor skill learning. *Neuron* 72: 443–454, 2011. doi:10.1016/j.neuron.2011.10.008.

de Werd MME, Boelen D, Rikkert MGMO, Kessels RPC. Errorless learning of everyday tasks in people with dementia. *Clin Interv Aging* 8: 1177–1190, 2013. doi:10.2147/CIA.S46809.

Di Lazzaro V, Ziemann U. The contribution of transcranial magnetic stimulation in the functional evaluation of microcircuits in human motor cortex. *Front Neural Circuits* 7: 18, 2013. doi:10.3389/fncir.2013.00018.

Donchin O, Francis JT, Shadmehr R. Quantifying generalization from trial-by-trial behavior of adaptive systems that learn with basis functions: theory and experiments in human motor control. *J Neurosci* 23: 9032–9045, 2003. doi:10.1523/JNEUROSCI.23-27-09032.2003.

Fusi S, Asaad WF, Miller EK, Wang X-J. A neural circuit model of flexible sensorimotor mapping: learning and forgetting on multiple timescales. *Neuron* 54: 319–333, 2007. doi:10.1016/j.neuron.2007.03.017.

Galea JM, Vazquez A, Pasricha N, de Xivry JJ, Celnik P. Dissociating the roles of the cerebellum and motor cortex during adaptive learning: the motor cortex retains what the cerebellum learns. *Cereb Cortex* 21: 1761–1770, 2011. doi:10.1093/cercor/bhq246.

Garvey MA, Ziemann U, Becker DA, Barker CA, Bartko JJ. New graphical method to measure silent periods evoked by transcranial magnetic stimulation. *Clin Neurophysiol* 112: 1451–1460, 2001. doi:10.1016/S1388-2457(01)00581-8.

Hadipour-Niktarash A, Lee CK, Desmond JE, Shadmehr R. Impairment of retention but not acquisition of a visuomotor skill through time-dependent disruption of primary motor cortex. *J Neurosci* 27: 13413–13419, 2007. doi:10.1523/JNEUROSCI.2570-07.2007.

Hallett M. Transcranial magnetic stimulation: a primer. *Neuron* 55: 187–199, 2007. doi:10.1016/j.neuron.2007.06.026.

Hamada M, Galea JM, Di Lazzaro V, Mazzone P, Ziemann U, Rothwell JC. Two distinct interneuron circuits in human motor cortex are linked to different subsets of physiological and behavioral plasticity. *J Neurosci* 34: 12,837–12,849, 2014. doi:10.1523/JNEUROSCI.1960-14.2014.

Hess G, Donoghue JP. Long-term potentiation of horizontal connections provides a mechanism to reorganize cortical motor maps. *J Neurophysiol* 71: 2543–2547, 1994. doi:10.1152/jn.1994.71.6.2543.

Howard IS, Ingram JN, Wolpert DM. A modular planar robotic manipulandum with end-point torque control. *J Neurosci Methods* 181: 199–211, 2009. doi:10.1016/j.jneumeth.2009.05.005.

Huberdeau DM, Krakauer JW, Haith AM. Dual-process decomposition in human sensorimotor adaptation. *Curr Opin Neurobiol* 33: 71–77, 2015. doi:10.1016/j.conb.2015.03.003.

Izawa J, Criscimagna-Hemminger SE, Shadmehr R. Cerebellar contributions to reach adaptation and learning sensory consequences of action. *J Neurosci* 32: 4230–4239, 2012. doi:10.1523/JNEUROSCI.6353-11.2012.

Joiner WM, Smith MA. Long-term retention explained by a model of short-term learning in the adaptive control of reaching. *J Neurophysiol* 100: 2948–2955, 2008. doi:10.1152/jn.90706.2008.

Keel JC, Smith MJ, Wassermann EM. A safety screening questionnaire for transcranial magnetic stimulation. *Clin Neurophysiol* 112: 720, 2001. doi:10.1016/S1388-2457(00)00518-6.

Kim S, Ogawa K, Lv J, Schweighofer N, Imamizu H. Neural substrates related to motor memory with multiple timescales in sensorimotor adaptation. *PLoS Biol* 13: e1002312, 2015. doi:10.1371/journal.pbio.1002312.

Kishore A, Meunier S, Popa T. Cerebellar influence on motor cortex plasticity: behavioral implications for Parkinson's disease. *Front Neurol* 5: 68, 2014. doi:10.3389/fneur.2014.00068.

Kojima S, Onishi H, Sugawara K, Kirimoto H, Suzuki M, Tamaki H. Modulation of the cortical silent period elicited by single- and paired-pulse transcranial magnetic stimulation. *BMC Neurosci* 14: 43, 2013. doi:10.1186/1471-2202-14-43.

Kojima Y, Iwamoto Y, Yoshida K. Memory of learning facilitates saccadic adaptation in the monkey. *J Neurosci* 24: 7531–7539, 2004. doi:10.1523/JNEUROSCI.1741-04.2004.

Krakauer JW, Pine ZM, Ghilardi MF, Ghez C. Learning of visuomotor transformations for vectorial planning of reaching trajectories. *J Neurosci* 20: 8916–8924, 2000. doi:10.1523/JNEUROSCI.20-23-08916.2000.

Lee J-Y, Schweighofer N. Dual adaptation supports a parallel architecture of motor memory. *J Neurosci* 29: 10396–10404, 2009. doi:10.1523/JNEUROSCI.1294-09.2009.

Mandelblat-Cerf Y, Novick I, Vaadia E. Expressions of multiple neuronal dynamics during sensorimotor learning in the motor cortex of behaving monkeys. *PLoS One* 6: e21626, 2011. doi:10.1371/journal.pone.0021626.

Maschke M, Gomez CM, Ebner TJ, Konczak J. Hereditary cerebellar ataxia progressively impairs force adaptation during goal-directed arm movements. *J Neurophysiol* 91: 230–238, 2004. doi:10.1152/jn.00557.2003.

McDonnell MN, Ridding MC. Transient motor evoked potential suppression following a complex sensorimotor task. *Clin Neurophysiol* 117: 1266–1272, 2006. doi:10.1016/j.clinph.2006.02.008.

Monfils M-H, VandenBerg PM, Kleim JA, Teskey GC. Long-term potentiation induces expanded movement representations and dendritic hypertrophy in layer V of rat sensorimotor neocortex. *Cereb Cortex* 14: 586–593, 2004. doi:10.1093/cercor/bhh020.

Oldfield RC. The assessment and analysis of handedness: the Edinburgh inventory. *Neuropsychologia* 9: 97–113, 1971. doi:10.1016/0028-3932(71)90067-4.

Rábago CA, Lancaster JL, Narayana S, Zhang W, Fox PT. Automated-parameterization of the motor evoked potential and cortical silent period

induced by transcranial magnetic stimulation. *Clin Neurophysiol* 120: 1577–1587, 2009. doi:10.1016/j.clinph.2009.04.020.

Rioult-Pedotti MS, Friedman D, Donoghue JP. Learning-induced LTP in neocortex. *Science* 290: 533–536, 2000. doi:10.1126/science.290.5491.533.

Rodi Z, Springer C. Influence of muscle contraction and intensity of stimulation on the cutaneous silent period. *Muscle Nerve* 43: 324–328, 2011. doi:10.1002/mus.21868.

Rossini PM, Burke D, Chen R, Cohen LG, Daskalakis Z, Di Iorio R, Di Lazzaro V, Ferreri F, Fitzgerald PB, George MS, Hallett M, Lefaucheur JP, Langguth B, Matsumoto H, Miniussi C, Nitsche MA, Pascual-Leone A, Paulus W, Rossi S, Rothwell JC, Siebner HR, Ugawa Y, Walsh V, Ziemann U. Non-invasive electrical and magnetic stimulation of the brain, spinal cord, roots and peripheral nerves: basic principles and procedures for routine clinical and research application. An updated report from an I.F.C.N. Committee. *Clin Neurophysiol* 126: 1071–1107, 2015. doi:10.1016/j.clinph.2015.02.001.

Scheidt RA, Dingwell JB, Mussa-Ivaldi FA. Learning to move amid uncertainty. *J Neurophysiol* 86: 971–985, 2001. doi:10.1152/jn.2001.86.2.971.

Scheidt RA, Reinkensmeyer DJ, Conditt MA, Rymer WZ, Mussa-Ivaldi FA. Persistence of motor adaptation during constrained, multi-joint, arm movements. *J Neurophysiol* 84: 853–862, 2000. doi:10.1152/jn.2000.84.2.853.

Schutter DJLG, van Honk J. A standardized motor threshold estimation procedure for transcranial magnetic stimulation research. *J ECT* 22: 176–178, 2006. doi:10.1097/01.yct.0000235924.60364.27.

Seidler RD, Noll DC. Neuroanatomical correlates of motor acquisition and motor transfer. *J Neurophysiol* 99: 1836–1845, 2008. doi:10.1152/jn.01187.2007.

Shadmehr R, Mussa-Ivaldi FA. Adaptive representation of dynamics during learning of a motor task. *J Neurosci* 14: 3208–3224, 1994. doi:10.1523/JNEUROSCI.14-05-03208.1994.

Sing GC, Smith MA. Reduction in learning rates associated with anterograde interference results from interactions between different timescales in motor adaptation. *PLOS Comput Biol* 6: e1000893, 2010. doi:10.1371/journal.pcbi.1000893.

Smith MA, Ghazizadeh A, Shadmehr R. Interacting adaptive processes with different timescales underlie short-term motor learning. *PLoS Biol* 4: e179, 2006. doi:10.1371/journal.pbio.0040179.

Spampinato D, Celnik P. Temporal dynamics of cerebellar and motor cortex physiological processes during motor skill learning. *Sci Rep* 7: 40715, 2017. doi:10.1038/srep40715.

Taylor JA, Ivry RB. Cerebellar and prefrontal cortex contributions to adaptation, strategies, and reinforcement learning. *Prog Brain Res* 210: 217–253, 2014. doi:10.1016/B978-0-444-63356-9.00009-1.

Taylor JL, Butler JE, Allen GM, Gandevia SC. Changes in motor cortical excitability during human muscle fatigue. *J Physiol* 490: 519–528, 1996. doi:10.1113/jphysiol.1996.sp021163.

Terao Y, Ugawa Y. Basic mechanisms of TMS. *J Clin Neurophysiol* 19: 322–343, 2002. doi:10.1097/00004691-200208000-00006.

Thoroughman KA, Shadmehr R. Learning of action through adaptive combination of motor primitives. *Nature* 407: 742–747, 2000. doi:10.1038/35037588.

Trewartha KM, Garcia A, Wolpert DM, Flanagan JR. Fast but fleeting: adaptive motor learning processes associated with aging and cognitive decline. *J Neurosci* 34: 13411–13421, 2014. doi:10.1523/JNEUROSCI.1489-14.2014.

van den Wildenberg WPM, Burle B, Vidal F, van der Molen MW, Ridderinkhof KR, Hasbroucq T. Mechanisms and dynamics of cortical motor inhibition in the stop-signal paradigm: a TMS study. *J Cogn Neurosci* 22: 225–239, 2010. doi:10.1162/jocn.2009.21248.

Werhahn KJ, Fong JK, Meyer BU, Priori A, Rothwell JC, Day BL, Thompson PD. The effect of magnetic coil orientation on the latency of surface EMG and single motor unit responses in the first dorsal interosseous muscle. *Electroencephalogr Clin Neurophysiol* 93: 138–146, 1994. doi:10.1016/0168-5597(94)90077-9.

Ziemann U. TMS and drugs. *Clin Neurophysiol* 115: 1717–1729, 2004. doi:10.1016/j.clinph.2004.03.006.

Ziemann U, Paulus W, Nitsche MA, Pascual-Leone A, Byblow WD, Berardelli A, Siebner HR, Classen J, Cohen LG, Rothwell JC. Consensus: motor cortex plasticity protocols. *Brain Stimul* 1: 164–182, 2008. doi:10.1016/j.brs.2008.06.006.

Ziemann U, Siebner HR. Modifying motor learning through gating and homeostatic metaplasticity. *Brain Stimul* 1: 60–66, 2008. doi:10.1016/j.brs.2007.08.003.